Eur Spine J (2008) 17:948–955
DOI 10.1007/s00586-008-0682-1

ORIGINAL ARTICLE

Cerebral glucose metabolic abnormality in patients with congenital scoliosis

Weon Wook Park · Kuen Tak Suh · Jeung Il Kim · Ja Gyung Ku · Hong Seok Lee · Seong-Jang Kim · In-Ju Kim · Yong-Ki Kim · Jung Sub Lee

Received: 27 November 2007 / Revised: 17 February 2008 / Accepted: 14 April 2008 / Published online: 30 April 2008

Abstract A possible association between congenital scoliosis and low mental status has been recognized, but there are no reports describing the mental status or cerebral metabolism in patients with congenital scoliosis in detail. We investigated the mental status using a mini-mental status exam as well as the cerebral glucose metabolism using F-18 fluorodeoxyglucose brain positron emission tomography in 12 patients with congenital scoliosis and compared them with those of 14 age-matched patients with adolescent idiopathic scoliosis. The mean mini-mental status exam score in the congenital scoliosis group was significantly lower than that in the adolescent idiopathic scoliosis group. Group analysis found that various brain areas of patients with congenital scoliosis showed glucose hypometabolisms in the left prefrontal cortex (Brodmann area 10), right orbitofrontal cortex (Brodmann area 11), left dorsolateral prefrontal cortex (Brodmann area 9), left anterior cingulate gyrus (Brodmann area 24) and pulvinar of the left thalamus. From this study, we could find the metabolic abnormalities of brain in patients with congenital scoliosis and suggest the possible role of voxel-based analysis of brain fluorodeoxyglucose positron emission tomography.

Keywords Congenital scoliosis · Mental status · Cerebral glucose metabolism · F-18 fluorodeoxyglucose · Positron emission tomography

Introduction

Congenital scoliosis (CS) can be associated with congenital abnormalities that can affect multiple organ systems or lead to acquired medical problems and morbidity as the child grows or while the spinal deformity is being treated. Common associated conditions of CS are cardiac abnormalities, urological abnormalities and spinal cord abnormalities. CS is associated with intraspinal anomalies in approximately 20% of patients and should be examined using magnetic resonance imaging [6, 11, 26]. Bradford et al. [3] reported that 38% of the 42 patients in their study had an intraspinal anomaly using magnetic resonance imaging. Using intravenous urography, MacEwen et al. [18] identified genitourinary abnormalities in 20% of patients with CS. The precise incidence of congenital heart disease associated with CS has not been reported. Basu et al. [2] found congenital heart disease in 26% of patients with a congenital spinal deformity.

Congenital scoliosis might be associated with a low mental status. Mental retardation is often observed in patients of CS associated with syndrome [16]. Although a possible association between CS and a low mental status has been recognized, we are not aware of any report describing the mental status or cerebral metabolism in patients with CS in detail. Therefore, we investigated the mental status and cerebral glucose metabolism in patients

W. W. Park · J. G. Ku
Department of Orthopaedic Surgery, Korea Hospital, Pusan, South Korea

K. T. Suh · J. I. Kim · H. S. Lee · J. S. Lee (✉)
Department of Orthopaedic Surgery, Medical Research Institute, Pusan National University School of Medicine, 1-10 Ami-Dong, Seo-Gu, Pusan 602-739, South Korea
e-mail: jungsublee@pusan.ac.kr

S.-J. Kim · I.-J. Kim · Y.-K. Kim
Department of Nuclear Medicine, Medical Research Institute, Pusan National University School of Medicine, Pusan, South Korea

with CS and compared the results with those from patients with adolescent idiopathic scoliosis (AIS).

Materials and methods

Subjects

We studied 12 CS and 14 AIS patients who had been admitted to our department for the surgical correction of scoliosis. The Cobb angles of the curves were measured on plain radiographs and the Risser signs were determined. All patients aged between 11 and 16 years presenting to the scoliosis were asked to voluntarily examine a mini-mental status examination [13] and an analysis of their cerebral glucose metabolism. Fourteen AIS patients were used as the control group because the cerebral glucose metabolism was reported to be similar to normal healthy controls [21]. All subjects were right-handed and had at least 5 years of education.

All subjects were also examined clinically to rule out any hidden metabolic disease, chromosomal abnormality, or psychiatric disease that could affect the cerebral glucose metabolism before entering the study. In addition, brain MR imaging studies were performed in all subjects before entering the study in order to rule out any organic brain lesion. Subjects with a history of neuromuscular disease, endocrine disease, skeletal dysplasia, connective tissue abnormalities, organic brain disease, psychiatric disease or other systemic congenital abnormality were excluded from the study. All subjects and their parents provided informed consent before the examination and measurements. The study was approved by the Clinical Research Ethics Committee of the university and the hospital.

F-18 FDG brain PET

Brain positron emission tomography (PET) scans of a single frame of 15 min were acquired starting 60 min after the intravenous injection of 370 MBq (10 mCi) F-18 fluorodeoxyglucose (FDG) per 1.7 m^2 of body surface area using a Gemini PET/CT scanner (Philips, Milpitas, CA, USA). It was performed with the subjects under resting conditions with their eyes closed and ears unplugged, comfortably lying in a darkened and quiet room. Subjects were fasted for at least 8 h before PET imaging. The PET images were reconstructed using 3D RAMLA (2 repetition, 0.006 relaxation parameter) and displayed in a 128 × 128 matrix (pixel size = 2 × 2 mm, with a slice thickness of 2 mm). Attenuation correction was performed with a uniform attenuation coefficient ($\mu = 0.096\ cm^{-1}$). In-plane and axial resolution of the scanner were 4.2 and 5.6 mm full width at half maximum (FWHM), respectively.

SPM analysis of regional cerebral glucose metabolism

Spatial preprocessing and statistical analysis were performed using the SPM2 implemented in Matlab 5.3 (The MathWorks, Inc., Natick, MA, USA). All the reconstructed F-18-FDG brain PET images were spatially normalized into Montreal Neurological Institute (MNI, McGill University, Montreal, Que., Canada) standard templates by an affine transformation (12 parameters for rigid transformations) and a non-linear transformation, then smoothed with a FWHM 8-mm Gaussian kernel to increase the signal-to-noise ratio and to account for subtle variations in anatomic structures. To remove the effects of the difference in the overall counts, the voxel counts were normalized to the mean voxel count of the gray matter in each PET image using proportional scaling. Images of the patients with CS were compared with those with AIS in a voxel-wise manner using SPM2 for between-group analysis ($P < 0.001$, uncorrected; extent threshold, $k = 50$). The clusters that passed this threshold were considered significant at $P < 0.05$ corrected for multiple comparisons. The Talairach brain coordinates were estimated from a non-linear transformation from MNI space to Talairach space (Talairach Daemon Client, Version 1.1, Research Imaging Center, University of Texas Health Science Center at San Antonio). The differences between the CS and AIS patients were examined using an extent threshold level of 50 voxels with a P value < 0.001 to illustrate the group differences in statistical voxel-based analysis, as well as for illustrating the result of the registration between CS and AIS. For the visualization of the t-score statistics (SPM{t} map), significant voxels were projected onto the three-dimensional rendered brain or a standard high-resolution MR image template provided by SPM2, thereby allowing anatomic identification. In addition, linear correlations of the regional brain glucose metabolism with the MMSE scores were investigated using 'single subject: covariates only' analysis and simple regression analysis, which are statistical models in SPM2 based on the general linear model. We looked for all voxels where the regional cerebral glucose metabolism was significantly and positively correlated with the MMSE scores. After group analysis, each F-18 FDG brain PET images of the CS patient was compared with those of the AIS patients to investigate individual brain glucose metabolism abnormalities using t statistics in SPM2.

Statistical analysis

Statistical analysis was performed with SPSS 11.5 software for Windows (SPSS, Chicago, IL, USA). Data were expressed by mean ± standard deviation. Groups were compared by using the Mann–Whitney U test. A $P \leq 0.05$ was regarded as statistically significant.

Results

Patients characteristics

Table 1 shows the details of the subjects. The CS group consisted of 12 patients (6 girls and 6 boys) with a mean age of 13.0 ± 1.4 years. The mean Cobb's angle of the major curve in the CS group was 50.2 ± 12.7 and the mean MMSE score was 22.4 ± 5.7. The AIS group consisted of 14 patients (10 girls and 4 boys) with a mean age of 13.2 ± 0.8 years. The mean MMSE score in the AIS group was 29.1 ± 1.1. The mean MMSE score was significantly lower in the CS group than in the AIS group ($P < 0.01$).

Group analysis of regional cerebral metabolism abnormalities by SPM analysis

As shown in Fig. 1 and Table 2, several voxel clusters of significantly decreased cerebral metabolism were observed in the CS patients using t-statistics. The largest cluster was an area of the left prefrontal cortex (Brodmann area 10) (voxel number 585, peak Z value = 3.30, uncorrected $P < 0.001$). The second largest cluster area was the right orbitofrontal cortex (Brodmann area 11) (voxel number 141, peak Z value = 3.11, uncorrected $P = 0.001$). The third largest cluster area was the left dorsolateral prefrontal cortex (Brodmann area 9) (voxel number 119, peak Z value = 3.36, uncorrected $P = 0.003$). The other clusters were the left anterior cingulate gyrus (Brodmann area 24) (voxel number 105, peak Z value = 2.98, 2.54 uncorrected $P = 0.001$) and pulvinar of the left thalamus (voxel number 72, peak Z value = 2.70, uncorrected $P = 0.001$).

Correlation of MMSE and brain metabolism

Positive correlations between the MMSE score and cerebral glucose metabolism were observed in several areas (Fig. 2). These areas were left basolateral prefrontal cortex (BA 44, peak $Z = 3.65$, MNI coordinate; −52, 16, 16, $P = 0.001$, $R^2 = 0.8247$), right prefrontal cortex (BA 10,

Table 1 Details of the subjects

Case	Age	Gender	Risser stage	Cobb's angle[a]	MMSE score	Diagnosis
1	14.3	M	3	41/LTL	25	Congenital scoliosis (T12 hemivertebra)
2	12.1	M	3	46/RTL	28	Congenital scoliosis (T12, L1 hemivertebra)
3	10.8	F	2	64/LL	11	Congenital scoliosis (L1, L2 hemivertebra)
4	11.8	M	2	39/RTL	24	Congenital scoliosis (T11 hemivertebra)
5	12.0	F	2	50/LTL	17	Congenital scoliosis (L1 hemivertebra)
6	15.2	M	3	55/LTL	13	Congenital scoliosis (multiple hemivertebra)
7	14.2	F	3	53/LTL	24	Congenital scoliosis (unilateral bar)
8	12.2	F	2	42/LL	25	Congenital scoliosis (L3 hemivertebra)
9	12.0	M	2	83/LT	22	Congenital scoliosis (unilateral bar)
10	14.6	M	3	46/LTL	26	Congenital scoliosis (T12 hemivertebra)
11	14.2	F	3	40/RT	27	Congenital scoliosis (multiple hemivertebra)
12	12.6	F	2	43/LL	27	Congenital scoliosis (L2 hemivertebra)
13	14.1	M	3	59/44/RT/LTL	30	Adolescent idiopathic scoliosis
14	13.2	F	3	55/41/RT/LTL	27	Adolescent idiopathic scoliosis
15	11.6	F	2	46/RT	29	Adolescent idiopathic scoliosis
16	12.5	F	2	57/39/RT/LTL	30	Adolescent idiopathic scoliosis
17	13.8	M	3	48/LTL	29	Adolescent idiopathic scoliosis
18	13.3	M	3	69/RT	30	Adolescent idiopathic scoliosis
19	12.5	F	2	38/59/RT/LL	30	Adolescent idiopathic scoliosis
20	12.0	F	2	62/RT	29	Adolescent idiopathic scoliosis
21	14.2	F	3	51/38/RT/LTL	30	Adolescent idiopathic scoliosis
22	13.5	F	2	60/43/RT/LTL	27	Adolescent idiopathic scoliosis
23	13.1	M	3	59/48/RT/LTL	30	Adolescent idiopathic scoliosis
24	13.6	F	4	48/62/RT/LL	29	Adolescent idiopathic scoliosis
25	12.7	F	2	48/49/RT/LTL	28	Adolescent idiopathic scoliosis
26	14.2	F	4	53/68/RT/LL	30	Adolescent idiopathic scoliosis

[a] *LTL* left thoracolumbar, *RTL* right thoracolumbar, *LL* left lumbar, *LT* left thoracic, *RT* right thoracic

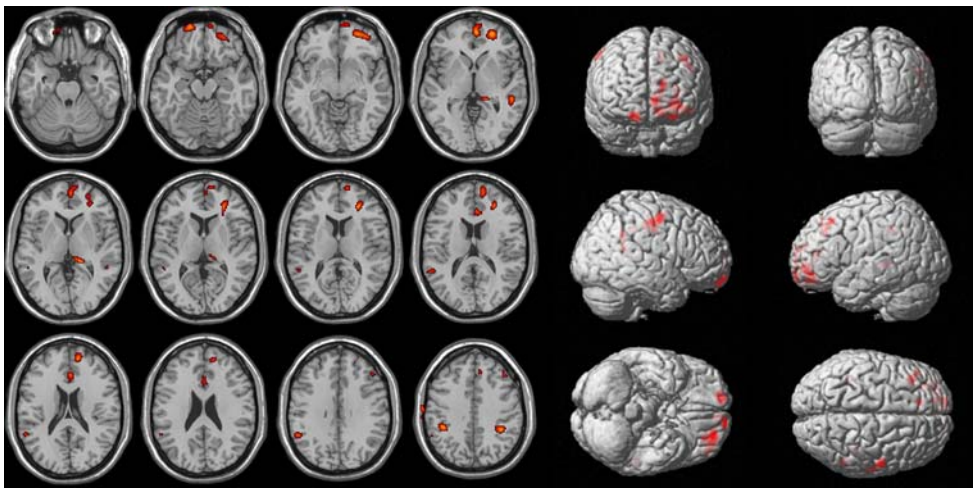

Fig. 1 Hypometabolic regions in the CS patients vs. AIS subjects. These regions are displayed on the axial (*left*) and surface rendered (*right*) images. Brain regions of the abnormal glucose metabolism are displayed using a height threshold of uncorrected $P = 0.001$ and an extent threshold of 50 voxels

Table 2 Group analysis results of brain areas of significantly decreased glucose metabolism in patients with CS compared to AIS

Cluster size	Hemisphere	Talairach coordinates			Peak *Z*	Structure	BA
		X	*Y*	*Z*			
585	Left	−26	54	−2	3.83	Prefrontal cortex	10
141	Right	16	62	−18	3.11	Orbitofrontal cortex	11
119	Left	−46	32	38	2.77	Dorsolateral prefrontal cortex	9
105	Left	−6	32	18	2.98	Anterior cingulate	24
	Left	−2	22	26	2.54	Anterior cingulate	24
72	Left	−18	−34	4	2.70	Thalamus, pulvinar	

BA Brodmann area

peak $Z = 3.86$, MNI coordinate; 8, 66, 0, $P = 0.0013$, $R^2 = 0.8222$), left middle temporal gyrus (BA 21, peak $Z = 3.76$, MNI coordinate; −62, −40, 0, $P = 0.0012$, $R^2 = 0.8216$), left middle frontal gyrus (BA 8, peak $Z = 3.57$, MNI coordinate; −24, 24, 48, $P \leq 0.001$, $R^2 = 0.8204$), left anterior cingulate (BA 32, peak $Z = 3.31$, MNI coordinate; −4, 48, 2, $P \leq 0.001$, $R^2 = 0.7869$), left dorsal posterior cingulate (BA 31, peak $Z = 3.16$, MNI coordinate; −8, −72, 22, $P \leq 0.001$, $R^2 = 0.8256$), left premotor cortex (BA 6, peak $Z = 3.14$, MNI coordinate; −34, −6, 54, $P \leq 0.001$, $R^2 = 0.6448$), right superior temporal gyrus (BA 22, peak $Z = 3.12$, MNI coordinate; 58, −44, 4, $P \leq 0.001$, $R^2 = 0.7786$), left lingual gyrus (BA 18, peak $Z = 3.11$, MNI coordinate; −12, −100, −12, $P \leq 0.001$, $R^2 = 0.6364$), and right anterior cingulate (BA 32, peak $Z = 3.10$, MNI coordinate; 10, 42, 16, $P \leq 0.001$, $R^2 = 0.7045$).

Individual analysis of regional cerebral metabolism abnormalities by SPM analysis

Table 3 demonstrates the SPM2 results of cerebral glucose metabolism in the individual CS patients compared to AIS.

Discussion

There are a number of reports for associated conditions of CS. These include cardiac abnormalities, urological abnormalities and spinal cord abnormalities. In addition, mental retardation is often observed in patients of CS associated with syndrome [16]. Despite a possible association between CS and a low mental status, reports about the mental status or cerebral metabolism in patients with CS are lacking. Therefore, we investigated the mental status and cerebral glucose metabolism in patients with CS. To our knowledge, this is the first report on the cerebral metabolism using F-18 FDG brain PET in patients with CS.

In this study, we determined a regional pattern of cerebral glucose metabolism in patients with CS using objective SPM analysis method. Because most of the patient group was adolescent, the ideal control group for SPM analysis would be age and gender matched group of normal adolescent. However, ethnical problems prohibit this. The rationale for using AIS as control group is based on our previous results showing similar cerebral glucose metabolism in AIS patients and normal young adults [21]. In this study, SPM was adopted for objective evaluation of

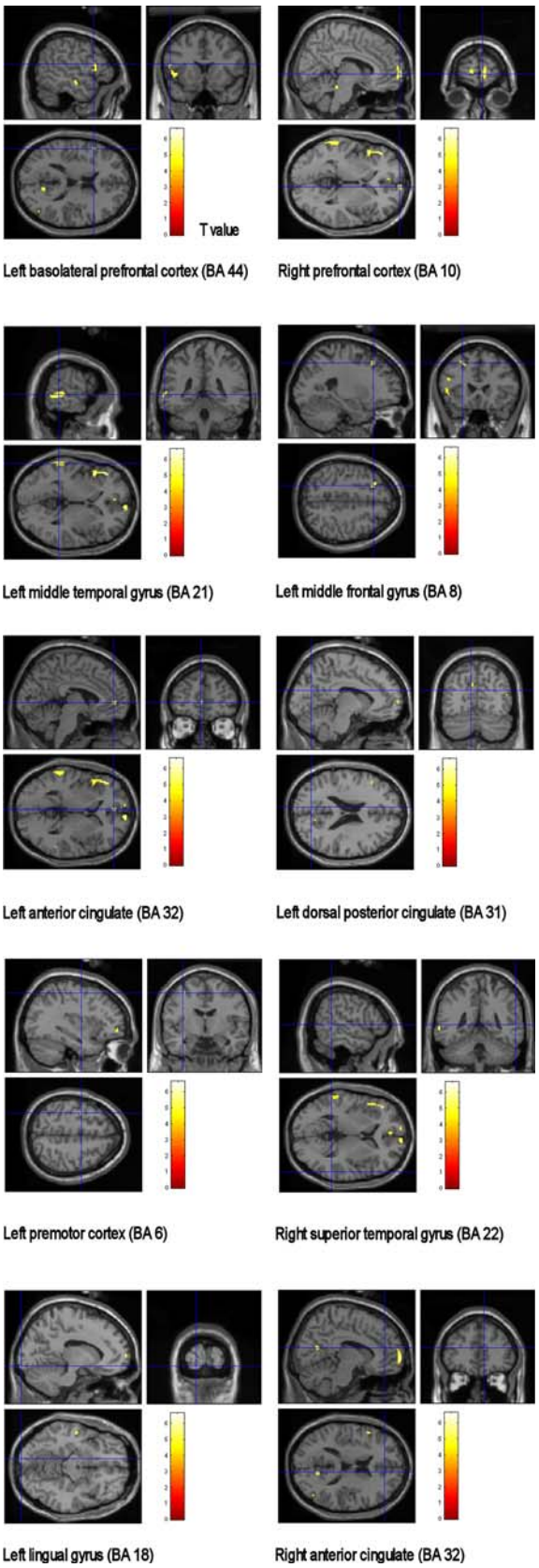

Fig. 2 Positive correlated brain areas in the patients with CS between MMSE scores and glucose metabolism

brain perfusion SPECT. The process of spatial normalization enables a voxel-based statistical comparison of brain images with different morphologies. SPM could allow the identification of abnormalities on an individual case-by-case basis, as well as group comparisons for different categories of brain diseases such as cognitive disorders, epilepsy and cerebrovascular diseases.

The group analysis found that various brain areas of the patients with CS showed glucose hypometabolisms in the left prefrontal cortex (Brodmann area 10), right orbitofrontal cortex (Brodmann area 11), left dorsolateral prefrontal cortex (Brodmann area 9), left anterior cingulate gyrus (Brodmann area 24) and pulvinar of the left thalamus. Those regions were correlated with cognitive and intellectual function. The overall decline in the cognitive function is closely correlated with the degree of cortical metabolic dysfunction [10]. The prefrontal cortical abnormalities newly emerged as patients showed further cognitive deterioration [8]. Eidelberg et al [9] reported glucose hypometabolism in the orbitofrontal cortex in cognitively impaired patients. This study demonstrates decreased cerebral glucose metabolism of prefrontal cortex by group analysis. Compared with AIS, the dorsolateral prefrontal cortex and prefrontal cortex were hypometabolic state.

The cingulate gyrus is the principal component of the limbic system, and its anterior and posterior parts possess different thalamic and cortical connections with different cytoarchitectures and subserve distinctive functions [12, 23]. The anterior cingulate gyrus can be divided into discrete anatomical and behavioral subdivisions: the affective division and the cognitive division [4]. The affective division includes the areas of Brodmann 25 and 33 and the rostal area of Brodmann 24, and plays a role in emotion and motivation. The cognitive division includes caudal areas of Brodmann 24 and 32 and plays a role in complex cognitive and attentional processing [4, 7, 24]. Previous study suggested that the major regions of age-related decline remain prominent in the prefrontal cortex as well as in the anterior cingulate gyrus [25].

The thalamus is also a principal component of the limbic system and the ascending reticular activating system. In addition, it is an input modulator where external sensory stimuli enter the cortex of the brain. Therefore, the thalamus has distinct connections with the cingulate gyrus, the reticular formation and the cerebral cortex. Decreased glucose metabolism in the thalamus is often observed in other studies regarding developmental disorders [17, 15]. From previous reports, it can be presumed that the thalamus plays an important role in brain development, especially in the early period of human life [5, 20].

From this study, CS patients might have some problems at the beginning period of brain development such as a

Table 3 Individual analysis results of brain areas of significantly decreased metabolism in patients with CS compared to AIS

Case	Hemisphere	Talairach coordinates			Peak *Z*	*P* value	Structure	BA
		X	*Y*	*Z*				
1	Right	38	62	4	3.07	0.033	Prefrontal cortex	10
	Left	−36	30	−8	2.92	0.04	Basolateral prefrontal cortex	47
	Right	58	−70	18	2.84	0.04	Middle temporal gyrus	39
2	Right	6	−20	10	3.27	0.035	Thalamus, medial dorsal nucleus	
	Left	−8	−28	8	3.25	0.031	Thalamus, pulvinar	
	Right	4	6	26	2.70	0.045	Corpus callosum	
	Left	−2	18	20	2.70	0.045	Anterior cingulate	
3	Left	0	−24	30	5.00	0.01	Cingulate gyrus	
	Left	−12	12	8	4.39	0.014	Caudate nucleus	
	Left	−14	−26	10	4.19	0.016	Thalamus, pulvinar	
	Left	−12	−38	−2	4.04	0.018	Parahippocampal gyrus	27
	Left	−52	−32	2	3.66	0.026	Superior temporal gyrus	22
	Left	−40	10	60	3.09	0.033	Middle frontal gyrus	6
	Left	−30	−14	−18	3.06	0.035	Hippocampus	
	Left	−16	56	40	3.01	0.038	Dorsolateral prefrontal cortex	9
	Left	−66	−36	−12	2.56	0.049	Middle temporal gyrus	21
4	Left	−2	56	−2	4.09	0.018	Prefrontal cortex	10
	Left	−16	38	18	2.68	0.045	Anterior cingulate	
	Right	54	−42	6	2.85	0.04	Superior temporal gyrus	22
	Right	4	22	40	3.00	0.038	Cigulate gyrus	32
	Right	64	0	0	2.95	0.04	Superior temporal gyrus	22
5	Right	2	−22	28	4.08	0.018	Cingulate gyrus	
	Right	60	12	−4	2.78	0.04	Superior temporal gyrus	22
	Right	58	−6	50	3.22	0.03	Precentral gyrus	6
	Right	24	−66	6	3.16	0.033	Posterior cingulate	30
	Left	−40	6	62	2.98	0.04	Middle frontal gyrus	6
6	Right	2	−24	28	3.67	0.026	Cingulate gyrus	
	Left	−20	−68	4	3.45	0.028	Posterior cingulate	30
	Right	52	−32	4	3.30	0.031	Superior temporal gyrus	22
	Right	16	−62	10	3.05	0.038	Posterior cingulate	
	Left	−14	−26	10	2.97	0.04	Thalamus, pulvimar	
7	Left	−18	−34	−8	5.13	0.01	Parahippocampal gyrus	
	Right	16	−62	10	4.51	0.01	Posterior cingulate	
	Left	−64	−34	28	4.44	0.01	Inferior parietal lobule	40
	Left	−64	−44	−2	3.84	0.02	Middle temporal gyrus	21
	Left	−30	−10	52	3.81	0.02	Precentral gyrus	6
	Left	−12	68	−6	3.46	0.028	Prefrontal cortex	10
	Right	12	68	2	3.41	0.028	Prefrontal cortex	10
	Right	2	−22	28	3.39	0.03	Cingulate gyrus	
	Right	10	−4	30	2.41	0.049	Cingulate gyrus	
	Left	−10	6	6	2.82	0.04	Caudate nucleus	
8	Left	−20	56	26	3.73	0.023	Prefrontal cortex	10
	Left	−54	2	−34	2.85	0.04	Middle temporal gyrus	21
	Left	−52	8	−22	2.82	0.04	Middle temporal gyrus	21
	Left	−32	24	42	3.10	0.033	Dorsolateral prefrontal cortex	9
9	Right	48	−30	46	3.70	0.023	Inferior parietal lobule	40
	Right	40	20	6	3.96	0.02	Insula	

Table 3 continued

Case	Hemisphere	Talairach coordinates			Peak *Z*	*P* value	Structure	BA
		X	*Y*	*Z*				
10	Left	−42	−42	40	3.53	0.026	Inferior parietal lobule	40
	Left	−4	−36	32	3.44	0.028	Cingulate gyrus	
	Right	8	−36	34	2.63	0.047	Cingulate gyrus	
	Left	12	−60	8	3.43	0.028	Posterior cingulate	
	Left	−52	−40	−20	2.97	0.04	Inferior temporal gyrus	37
	Left	−50	4	−36	2.94	0.04	Middle temporal gyrus	21
11	Right	24	−14	70	3.81	0.02	Premotor cortex	6
	Right	12	−12	72	3.27	0.031	Premotor cortex	6
	Left	−16	−12	72	3.67	0.026	Premotor cortex	6
	Left	−14	26	36	3.35	0.03	Dorsolateral prefrontal cortex	9
	Left	−16	28	28	3.09	0.033	Anterior cingulate	
	Left	−10	30	20	2.74	0.04	Anterior cingulate	
	Left	−50	−30	−2	2.62	0.047	Superior temporal gyrus	22
12	Left	−42	−4	46	4.11	0.016	Premotor cortex	6
	Right	52	−52	52	3.82	0.02	Inferior parietal lobule	40
	Left	−48	14	38	3.88	0.02	Dorsolateral prefrontal cortex	9
	Right	36	40	40	3.73	0.023	Dorsolateral prefrontal cortex	9
	Right	36	62	2	3.32	0.032	Prefrontal cortex	10

BA Brodmann area

congenital factor or a functional deficit in the subcortical areas including the thalamus, which can widely influence brain development and resulting in various developmental disorders.

The correlations between the cognitive function and cerebral glucose metabolism revealed that various brain areas had positive correlations between the MMSE scores and the cerebral glucose metabolism in this study, including the prefrontal cortex, anterior and posterior cingulate gyri, and premotor cortex. The posterior cingulate gyrus plays a role in orientation and interpretation of the environment [22, 23], and has connections and behavioral attributes distinct from those of the anterior cingulate gyrus. Therefore, the functions of these divisions are probably coordinated [12]. The posterior cingulate gyrus also has dense connections with the medial temporal memory system. These communications might play a role in the posterior cingulate gyrus in orientation [7].

Anatomically, the posterior cingulate gyrus and its adjacent medial parietal cortex connect to the anterior cingulate, prefrontal, lateral parietal, and temporal cortices, as demonstrated in a monkey model [19]; such anatomical findings indicate that the posterior cingulate area plays a role in orchestrating the multimodal associative functions. In a clinical setting, cerebral blood flow in the posterior cingulate has been shown to be correlated with the clinical severity of dementia [1], and long-term changes in the posterior cingulate cerebral blood flow could be predictive of an onset of clinical symptoms of Alzheimer disease later in life [14]. In line with these findings, the posterior cingulate glucose metabolism in our CS patients showed a positive correlation with the scores on the MMSE, which is a test of mixed cognitive-memory performance.

This study suggests the possible role of voxel-based analysis of brain FDG PET abnormalities in patients with CS. From this study, the metabolic abnormalities of the brain in patients with CS could be identified clearly using group and individual analyses of SPM2. However, the numbers of subjects in the subgroups examined was too small to allow a valid result with external variables such as age, gender or the neuropsychological test results. Therefore, more study on a larger number of patients will be needed to allow a more objective SPM analysis of patients with CS.

Acknowledgments W. W. Park and K. T. Suh contributed equally to this study. This study was supported for two years by Pusan National University Research Grant.

References

1. Alsop DC, Detre JA, Grossman M (2000) Assessment of cerebral blood flow in Alzheimer's disease by spin-labeled magnetic resonance imaging. Ann Neurol 47:93–100
2. Basu PS, Elsebaie H, Noordeen MH (2002) Congenital spinal deformity: a comprehensive assessment at presentation. Spine 27:2255–2259

3. Bradford DS, Heithoff KB, Cohen M (1991) Intraspinal abnormalities and congenital spine deformities: a radiographic and MRI study. J Pediatr Orthop 11:36–41
4. Bush G, Luu P, Posner MI (2000) Cognitive and emotional influences in anterior cingulate cortex. Trends Cogn Sci 4:215–222
5. Chiron C, Raynaud C, Maziere B, Zilbovicius M, Laflamme L, Masure MC, Dulac O, Bourguignon M (1992) Changes in regional cerebral blood flow during brain maturation in children and adolescents. J Nucl Med 33:696–703
6. Conner AN, Young DG, Hide TA (1984) Occult intraspinal anomalies and congenital scoliosis. J Bone Joint Surg 66:1319
7. Devinsky O, Morrell MJ, Vogt BA (1995) Contributions of anterior cingulate cortex to behaviour. Brain 118:279–306
8. Drzezga A, Lautenschlager N, Siebner H, Riemenschneider M, Willoch F, Minoshima S, Schwaiger M, Kurz A (2003) Cerebral metabolic changes accompanying conversion of mild cognitive impairment into Alzheimer's disease: a PET follow-up study. Eur J Nucl Med Mol Imaging 30:1104–1113
9. Eidelberg D, Moeller JR, Dhawan V, Sidtis JJ, Ginos JZ, Strother SC, Cedarbaum J, Greene P, Fahn S, Rottenberg DA (1990) The metabolic anatomy of Parkinson's disease: complementary [18F]fluorodeoxyglucose and [18F]fluorodopa positron emission tomographic studies. Mov Disord 5:203–213
10. Foster NL, Chase TN, Mansi L, Brooks R, Fedio P, Patronas NJ, Di Chiro G (1984) Cortical abnormalities in Alzheimer's disease. Ann Neurol 16:649–654
11. Gillespie R, Faithfull DK, Roth A, Hall JE (1973) Intraspinal anomalies in congenital scoliosis. Clin Orthop Relat Res 93:103–109
12. Hirono N, Mori E, Ishii K, Ikejiri Y, Imamura T, Shimomura T, Hashimoto M, yamashita H, Sasaki M (1998) Hypofunction in the posterior cingulate gyrus correlates with disorientation for time and place in Alzheimer's disease. J Neurol Neurosurg Psychiatry 64:552–554
13. Jeong SK, Cho KH, Kim JM (2004) The usefulness of the Korean version of modified mini-mental state examination (K-mMMSE) for dementia screening in community dwelling elderly people. BMC Public Health 4:31
14. Johnson KA, Jones K, Holman BL, Becker JA, Spiers PA, Satlin A, Albert MS (1998) Preclinical prediction of Alzheimer's disease using SPECT. Neurology 50:1563–1571
15. Lee JD, Kim DI, Ryu YH, Whang GJ, Park CI, Kim DG (1998) Technetium-99m-ECD brain SPECT in cerebral palsy: comparison with MRI. J Nucl Med 39:619–623
16. Lee CK, Chang BS, Hong YM, Yang SW, Lee CS, Seo JB (2001) Spinal deformities in Noonan syndrome: a clinical review of sixty cases. J Bone Joint Surg 83-A:1495–1502
17. Lee BF, Yang P, Jong YJ, Hsu HY, Chen CC (2002) Single photon emission computerized tomography in children with developmental language disorder-a preliminary report. Kaohsiung J Med Sci 18:373–378
18. MacEwen GD, Winter RB, Hardy JH (1972) Evaluation of kidney anomalies in congenital scoliosis. J Bone Joint Surg 54-A:1451–1454
19. Pandya DN, Van Hoesen GW, Mesulam MM (1981) Efferent connections of the cingulate gyrus in the rhesus monkey. Exp Brain Res 42:319–330
20. Rubinstein M, Denays R, Ham HR, Piepsz A, VanPachterbeke T, Haumont D, Noel P (1989) Functional imaging of brain maturation in humans using iodine-123 iodoamphetamine and SPECT. J Nucl Med 30:1982–1985
21. Suh KT, Lee SS, Kim SJ, Kim YK, Lee JS (2007) Pineal gland metabolism in patients with adolescent idiopathic scoliosis. J Bone Joint Surg 89-B:66–71
22. Sutherland RJ, Whishaw IQ, Kolb B (1988) Contributions of cingulate cortex to two forms of spatial learning and memory. J Neurosci 8:1863–1872
23. Vogt BA, Finch DM, Olson CR (1992) Functional heterogeneity in cingulate cortex: the anterior executive and posterior evaluative regions. Cereb Cortex 2:435–443
24. Whalen PJ, Bush G, McNally RJ, Wilhelm S, McInerney SC, Jenike MA, Rauch SL (1998) The emotional counting Stroop paradigm: a functional magnetic resonance imaging probe of the anterior cingulate affective division. Biol Psychiatry 44:1219–1228
25. Willis MW, Ketter TA, Kimbrell TA, George MS, Herscovitch P, Danielson AL, Benson BE, Post RM (2002) Age, sex and laterality effects on cerebral glucose metabolism in healthy adults. Psychiatry Res 114:23–37
26. Winter RB, Haven JJ, Moe JH, Lagaard SM (1974) Diastematomyelia and congenital spine deformities. J Bone Joint Surg 56-A:27–39